methods

# Biotinylated θ-toxin derivative as a probe to examine intracellular cholesterol-rich domains in normal and Niemann-Pick type C1 cells

**Shigeki Sugii,* Patrick C. Reid,* Nobutaka Ohgami,* Yukiko Shimada,** Robert A. Maue,† Haruaki Ninomiya,§ Yoshiko Ohno-Iwashita,** and Ta-Yuan Chang[1,*]**

Department of Biochemistry,* and Departments of Physiology and Biochemistry,† Dartmouth Medical School, Hanover, NH 03755; Department of Neurobiology,§ Tottori University Faculty of Medicine, Yonago 683-8503, Japan; and Biomembrane Research Group,** Tokyo Metropolitan Institute of Gerontology, 35-2 Sakae-cho, Itabashi-ku, Tokyo 173-0015, Japan

**Abstract BCθ is a proteolytically nicked and biotinylated derivative of a cholesterol binding protein perfringolysin O (θ-toxin), and has been used to detect cholesterol-rich domains at the plasma membrane (PM). Here we show that by modifying the cell fixation condition, BCθ can also be used to detect cholesterol-rich domains intracellularly. When cells were processed for PM cholesterol staining, the difference in BCθ signals between the CT43 (CT) cell, a mutant Chinese hamster ovary cell line lacking the Niemann-Pick type C1 (NPC1) protein, and its parental cell 25RA (RA) was minimal. However, when cells were fixed with 4% paraformaldehyde, they became permeable to BCθ. Under this condition, BCθ mainly stained cholesterol-rich domains inside the cells, with the signal being much stronger in CT cells than in RA cells. The sensitivity of BCθ staining was superior to that of filipin staining. The staining of cholesterol-rich domain(s) inside RA cells was sensitive to β-cyclodextrin treatment, while most of the staining inside CT cells was relatively resistant to cyclodextrin treatment. Clear differences in intracellular BCθ staining were also seen between the normal and mutant NPC1 fibroblasts of human or mouse origin. Thus, BCθ is a powerful tool for visually monitoring cholesterol-rich domains inside normal and NPC cells.**—Sugii, S., P. C. Reid, N. Ohgami, Y. Shimada, R. A. Maue, H. Ninomiya, Y. Ohno-Iwashita, and T-Y. Chang. **Biotinylated θ-toxin derivative as a probe to examine intracellular cholesterol-rich domains in normal and Niemann-Pick type C1 cells. *J. Lipid Res.* 2003.** 44: **1033–1041.**

**Supplementary key words** BC θ • perfringolysin O toxin • cholesterol metabolism • cholesterol stain • intracellular cholesterol trafficking • cholesterol mutants • lipid rafts

Microdomains called lipid rafts exist in all mammalian cell membranes. They are rich in cholesterol and sphingolipids, and play important roles in various cellular processes, including signal transduction, cell surface polarity, and endocytosis (1). In addition, it has been shown that cholesterol modulates intracellular transport of proteins from early endosomes to the plasma membranes (PMs), or from endosomes to the Golgi (2–4); it also modulates the trafficking pathway of other lipids such as sphingolipids (5, 6). At present, cellular factors that determine the concentration and the localization of cholesterol inside the cell remain largely unknown. One of the key molecules involved in the correct distribution of intracellular cholesterol is Niemann-Pick type C1 (NPC1) protein [mutation in *NPC1* causes NPC syndrome, a fatal pediatric neurodegenerative disease (7)]. Although the precise mechanism is still not clear, NPC1 was shown to mediate the transport of LDL-derived cholesterol from endosome/lysosome to the PM and to the endoplasmic reticulum (ER) (reviewed in ref. 8). Chinese hamster ovary (CHO) mutants that are defective in the NPC1 protein have been isolated and characterized (9–11). We compared the cholesterol trafficking activities between the NPC1 mutants [CT43 (CT) and CT60] and their parental cell line 25RA (RA) (12, 13), and showed that NPC1 also participates in the transport of PM-derived cholesterol to the ER. Cholesterol newly synthesized in the ER quickly moves to the PM. After arrival at the PM, its retrograde transport back to the ER for esterification has been shown to require NPC1 (14, 15). Similar findings have been reported by other investigators (16–18). These studies suggest that, irrespective of the origin of cholesterol, the lack

Abbreviations: CD, β-cyclodextrin; CHO, Chinese hamster ovary; ER, endoplasmic reticulum; GFP, green fluorescent protein; hpCD, 2-hydroxypropyl-β-cyclodextrin; LDLR, low density lipoprotein receptor; NPC1, Niemann-Pick type C1; PFA, paraformaldehyde; PM, plasma membrane.

[1] To whom correspondence should be addressed.
e-mail: ta.yuan.chang@dartmouth.edu

*Manuscript received 29 September 2002 and in revised form 5 December 2002.*

*Published, JLR Papers in Press, February 1, 2003.*
*DOI 10.1194/jlr.D200036-JLR200*

of a functional NPC1 protein invariably leads to cholesterol accumulation in the late endosome/lysosome.

For studying intracellular cholesterol transport, the biochemical approach is often problematic, partly because of the difficulty in isolating distinct subcellular organelles in their pure state. In recent years, the microscopic approach has provided invaluable information. One of the most frequently used methods for specifically viewing cholesterol-rich domains in intact cells is to label cholesterol by filipin, a naturally fluorescent polyene antibiotic that has a high affinity toward cholesterol (19). Several problems associated with the use of filipin for highlighting cholesterol in various tissues and cells have been noted in the literature (20–24), and are summarized as follows: *i*) the absorption spectrum of filipin is within the UV range (most of the confocal microscopes commercially available are not equipped with the laser beam that excites in the UV range); *ii*) the fluorescence signal of filipin bleaches in a short time; *iii*) in unfixed or fixed cells, filipin deforms the cellular membrane by forming complexes with cholesterol, and causes perturbation of membrane lipid organization; and *iv*) filipin has been reported to give false-negative results. Two fluorescent analogs of cholesterol, NBD cholesterol, and dehydroergosterol (DHE) have been used by various investigators to track the fate of unesterified sterol in the cell (25, 26). NBD cholesterol exhibits a strong initial fluorescence signal at desirable wavelengths, but bleaches quickly under light exposure. Moreover, NBD cholesterol may not faithfully mimic the behavior of cholesterol inside the cells (25). DHE was reported to behave in a manner similar to cholesterol in many ways (26), but its fluorescence intensity is weak (it absorbs and emits in the UV region, therefore special equipment is required in order to visualize it by fluorescence microscopy). For these reasons, there is a need to develop a reliable and versatile cholesterol-specific probe for microscopic studies.

Recently, a novel probe (BCθ) was developed as an effective tool for detecting cholesterol-rich domains (27, 28). The probe is derived from a pore-forming cytolysin produced by the pathogenic bacterium *Clostridium perfringens* (28). This thiol-activated cytolysin, called perfringolysin O (θ-toxin), specifically binds to free (unesterified) cholesterol (29–32) and forms oligomeric pores in the membranes (33). The probe BCθ was prepared by a two-step procedure. First, θ-toxin is proteolytically digested with subtilisin Carlsberg. This step generates a complex of 38 and 15 kDa fragments called Cθs (34). Next, the complex Cθ is biotinylated and purified, resulting in what is called BCθ (28). The biotinylation allows Cθ to be identified through binding to avidin. When used in fluorescence microscopy, the labeling efficiency of BCθ depends on the qualities of fluorescent avidin or streptavidin. Various kinds of avidin/streptavidin products with different fluophores, having stable fluorescent properties, are available, making this reagent suitable for double staining purposes. BCθ binds to cholesterol in synthetic liposomes and in intact cells with identical affinity to that of the wild-type (WT) θ-toxin, but because it does not oligomerize, it bears no hemolytic activity (28, 30, 31). Recently, it was demonstrated that BCθ binds to cholesterol-rich microdomains in the PM of intact cells with or without fixation (27, 35, 36).

BCθ is relatively high in molecular weight (~57 kDa) and has not been considered to be an effective agent for staining cholesterol inside the cells. In the current work, we show that increasing the concentration of paraformaldehyde (PFA) from 1% to 4% during the cell fixation step allows the entry of BCθ to stain cholesterol-rich domains inside mammalian cells. The signal elicited with BCθ staining is superior to that of filipin staining. This methodology was proven to be useful in studying cholesterol distribution in the NPC1-dependent manner.

## MATERIALS AND METHODS

### Materials

Filipin and 2-hydroxypropyl-β-cyclodextrin (hpCD) were purchased from Sigma. PFA was obtained from Sigma and from Electron Microscopy Sciences (Ft. Washington, PA) and gave the same results as described in this work. U18666A was from Biomol. FuGENE 6 Transfection Reagent was from Roche. ProLong Antifade Kit and Oregon Green 488-, Alexa 568-, or Texas Red-X-conjugated streptavidin were from Molecular Probes. LDL was prepared from fresh human plasma by sequential flotation as previously described (37).

### Preparation of BCθ

BCθ was prepared as previously described (27). Briefly, θ-toxin was overexpressed in *Escherichia coli* strains, and purified by a series of chromatographies (38). It was digested with subtilisin Carlsberg to produce a nicked θ-toxin (Cθ) (34). BCθ was then obtained by biotinylating Cθ as described (28).

### Cell lines

RA is a CHO cell line resistant to the cytotoxicity of 25-hydroxycholesterol (12) and contains a gain-of-function mutation in the sterol regulatory element binding protein-1 cleavage-activating protein (SCAP) (13). The CT mutant cell line is isolated as one of the cholesterol-trafficking mutants from mutagenized RA cells (9). It contains the same gain-of-function mutation in SCAP. In addition, it contains a premature translational termination mutation near the 3′ end of the *NPC1* coding sequence, producing a nonfunctional, truncated NPC1 protein (15). The human fibroblast cell line derived from an NPC patient (93. 22) was the generous gift of Dr. Peter Pentchev.

Isolation of mouse embryonic fibroblasts (MEFs) was performed as described (39). Briefly, at embryonic day 17, mouse embryos were taken out of the uteri of pregnant females from confirmed *npc1* heterozygous breeding pairs by caesarean section. For each embryo, the tail and a portion of a limb were removed and prepared for DNA extraction and genotyping according to the procedure described (40). After dissection and incubation in 0.05% trypsin solution, the softened tissue was disrupted by repeated pipetting. Cell debris was separated and the supernatant plated in T25 $cm^2$ flasks. Fibroblasts at early passages (fourth to tenth) were used in the current work. All experimental protocols were approved by the Institutional Animal Care and Research Advisory Committee at Dartmouth Medical School and conducted in accordance with the US Public Health Service guide for the care and use of laboratory animals.

### Cell culture

CHO cells were maintained in medium A [Ham's F-12, plus 10% fetal bovine serum (FBS) and 10 μg/ml gentamycin] as monolayers at 37°C with 5% $CO_2$. Medium D refers to Ham's F-12 with 5% delipidated FBS (41), plus 35 μM oleic acid and 10 μg/ml gentamycin. When medium D was used at lower temperatures (below 18°C), sodium bicarbonate was depleted from Ham's F-12 and cells were placed in the incubator without $CO_2$. Human fibroblasts and MEFs were grown in the same conditions as the CHO cells, except that Dulbecco's modified Eagle's medium and Pen-Strep (100 U/ml) were used.

### Construction and transfection of green fluorescent protein-tagged NPC1

A PCR fragment was generated using green fluorescent protein (GFP) cDNA as the template and a 5′ primer whose sequence corresponds to the C-terminal sequence of the mouse NPC1 from the unique *Eco*47III restriction site to the end of the reading frame (except the stop codon) followed by the sequence corresponding to six alanines (the spacer), which is in turn followed by a sequence corresponding to the N-terminal sequence of GFP (5′-TATATAAGCGCTACAGAGGGACAGAGAGAGAACGGCTCCTCAATTTTGCAGCAGCAGCAGCAGCAATGGTGAGCAAGGGCGAGGA-3′). The 3′ primer consists of sequences corresponding to the C-terminal sequence of GFP and to *Hind*III and *Xho*II restriction sites (5′-CGTCTGAAGCTTAGATCTTTACTTGTACAGCTCGTCCA-3′). The resulting PCR product was digested with *Hind*III and *Eco*47III and ligated into an NPC1-containing Bluescript plasmid that had been digested with *Eco*47III and *Hind*III and gel purified. The resulting cDNA encoding the NPC1-(ala)6-GFP fusion protein was sequenced on both strands to confirm that it was correct. The GFP-tagged NPC1 protein (NPC1-GFP) was removed from the plasmid with *Spe*I and *Hind*III and subcloned into the pREX-IRES vector (42). CT cells were transfected with the NPC1-GFP cDNA using FuGENE 6 according to manufacturer's instructions. Transfected cells were imaged within 2–3 days of transfection.

### Fluorescence microscopy

Cells were grown on glass coverslips in 6-well plates and processed for fluorescence studies. In some experiments, to minimize the possible effect of residual serum adhering to the coverslips, we incubated the cells in a serum-free medium for 2 h before the experiments and noticed no difference in results obtained with or without the preincubation step. For BCθ staining of fixed cells, the cells were washed three times and fixed with 4% or 1% PFA in PBS for 10 min or longer at room temperature. After extensive washes with PBS, the cells were preincubated in PBS containing 1% BSA, then 10 μg/ml BCθ in 1% BSA-PBS was added and incubated with the cells for 30 min at room temperature. After washing three times, the cells were incubated with either Oregon Green 488- or with Texas Red X-conjugated streptavidin (1 μg/ml) in PBS with 1% BSA at room temperature. After three washes, the coverslips were mounted with a drop of ProLong Anti-Fade media onto the glass plates for image processing. In the case of filipin staining, the protocol was essentially the same except that cells were preincubated with 1.5 mg/ml glycine in PBS for 30 min, then incubated with filipin (125 μg/ml) in PBS for 1 h at room temperature before image processing. For live-cell staining, cells were chilled and kept on ice, washed three times, preincubated in ice-cold phenol red-free Hank's balanced salt solution (HBSS) containing 1% BSA, then incubated with 10 μg/ml BCθ in the same solution for 30 min at 4°C. After washing three times with HBSS, the cells were incubated with fluorescent streptavidin in HBSS with 1% BSA at 4°C, and processed for image analysis. Samples were viewed and photographed using a Zeiss Axiophot microscope with a 63× objective equipped with CCD camera DEI-750 from Optronics Engineering (Goleta, CA). DAPI filter, FITC filter, and Texas Red filter were used to visualize filipin, GFP-Oregon Green 488, and Texas Red X, respectively. Using the MetaView 4.5 software from Universal Imaging Corp. (Downingtown, PA), we processed the images. To establish the validity of the localization studies, the BCθ-treated samples were labeled with Alexa 568-conjugated streptavidin and viewed with a Bio-Rad (Hercules, CA) MRC-1024 Krypton-Argon laser confocal microscope with 0.2 μm per optical section. The images were constructed by LaserSharp software, and further processed by Adobe Photoshop 5.02.

### Flow cytometry

Cells were processed for BCθ staining with Oregon Green 488-streptavidin essentially as described above except that the cells were grown without coverslips in 6-well dishes. After the staining, the cells were scraped by rubber policemen into microtubes, pelleted with a brief centrifugation, and resuspended in 1 ml of 1% BSA in either HBSS (for live-cell staining) or PBS (for fixed-cell staining). The cells were analyzed at excitation wavelength of 488 nm and emission wavelength of 515–530 nm using FACScan cytometer with CellQuest software (Becton Dickinson, San Jose, CA). Sorted for each sample were $10^4$ cells.

## RESULTS AND DISCUSSION

### Different fixation conditions produce different staining patterns

Due to its lack of hemolytic activity and its relatively large molecular weight, previous studies have focused on using BCθ for labeling cholesterol-rich microdomains at the PM of intact cells (27, 43). We used the RA cells and CT cells unfixed or fixed with low concentrations of PFA (1%), incubated them with BCθ followed by secondary staining using a fluorescent streptavidin, then viewed cells under a fluorescent microscope with confocal and differential interference contract (DIC) imaging capabilities.

TABLE 1. Flow cytometric analysis of BCθ staining under different fixation conditions

| Cell Line | Staining Method | Relative Mean Fluorescence Intensity[a] | % Cells in M1[b] range |
|---|---|---|---|
| 25RA | Live cell staining | 100 | 89.7 ± 5.4 |
| CT43 | | 109 ± 3 | 89.2 ± 6.1 |
| WT | | 76 ± 2 | 68.4 ± 4.6 |
| M19 | | 26 ± 19 | 24.8 ± 9.2 |
| 25RA | Fixation with 1% PFA | 100 | 5.7 ± 0.7 |
| CT43 | | 117 ± 7 | 9.5 ± 2.0 |
| WT | | 115 ± 5 | 5.8 ± 3.8 |
| M19 | | 23 ± 11 | 0.5 ± 0.3 |
| 25RA | Fixation with 4% PFA | 100 | 37.2 ± 4.2 |
| CT43 | | 154 ± 25 | 78.0 ± 4.6 |
| WT | | 82 ± 4 | 21.7 ± 11.4 |
| M19 | | 34 ± 8 | 2.8 ± 1.0 |

The data are combined results of three separate experiments. Values represent mean ± SD from three experiments.

[a] The data are expressed as percentages of the 25RA value for each staining method.

[b] M1 is defined as the region of fluorescence intensity that contains less than 0.1% of control cells (no BCθ incubation, with streptavidin only) for each staining method.

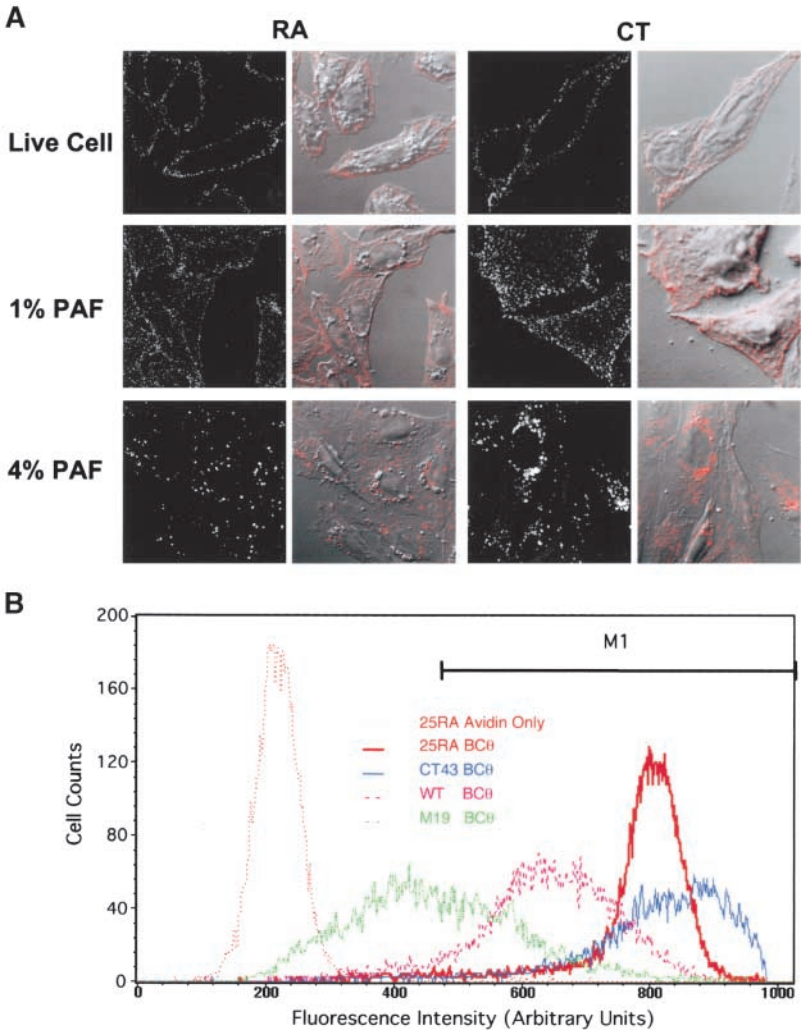


**Fig. 1.** A: Different staining methods produce distinct staining patterns in 25RA (RA) and CT43 (CT) cells. Monolayers of RA and CT cells were incubated with BCθ at 4°C without fixation (live cell), or fixed with 1% paraformaldehyde (PFA) or 4% PFA, then incubated with BCθ at room temperature. The treated cells were stained by incubating with Alexa 568 streptavidin at room temperature (for fixed cells) or at 4°C (for live cells), then viewed under confocal microscopy or differential interference contract (DIC) microscopy. To demonstrate localization of the fluorescent signals in the cell, the pictures with the DIC image were superimposed onto the pictures with the BCθ staining image. B: Flow cytometric analysis of BCθ staining to unfixed, live cells. Unfixed RA, CT, wild-type (WT), and M19 cells were incubated with BCθ at 4°C, followed by staining with Oregon Green 488 streptavidin at 4°C. As a negative control, cells were incubated with Oregon Green 488 streptavidin alone; only the result using RA is shown as a representative. M1 range is defined as the region of fluorescence intensity that contains less than 0.1% of the negative control cells.

To demonstrate localization of the fluorescent signals in the cells, the pictures with the DIC images were superimposed onto the pictures with the BCθ staining images.

As expected, treating unfixed or 1% PFA-fixed cells with BCθ resulted in strong staining mainly in the vicinity of the cell surface (**Fig. 1A**; 1st and 2nd rows). In addition, some intracellular staining signal(s) could also be observed, particularly in CT cells fixed with 1% PFA. Unexpectedly, when RA cells and CT cells were fixed with 4% PFA at room temperature for more than 10 min, we found that the intensity of cell surface staining was significantly reduced. The staining signals now mainly resided inside the cells, with higher intensities observed in CT cells than in RA cells (Fig. 1A; 3rd rows). It is known that NPC1 mutants accumulate a large amount of intracellular cholesterol. This result is thus consistent with the interpretation that under this condition, BCθ mainly stains intracellular cholesterol. Control experiments showed that no fluorescence signal was detectable in cells incubated with fluorescent streptavidin alone without BCθ (data not shown). We believe that the results seen in 4% PFA fixed cells were mainly due to increased permeability toward BCθ, allowing it to be accessible to cholesterol-rich domains in the cell interior. A similar observation was made by Hao and colleagues, who showed that, when treated with an intermediate concentration of PFA (2%), a significant percentage of the CHO cells became permeabilized to macromolecules, as judged by intracellular phalloidin staining (44).

The reduced cell surface staining by BCθ in cells treated with 4% PFA might be the consequence of deformation/reorganization of the PM, which in turn inhibited the binding between BCθ and cholesterol at the PM. [It is possible that the loss of cell surface BCθ staining signal after 4% PFA fixation may be due to redistribution of cholesterol from the PM to the internal membranes; however, this interpretation would not be compatible with the earlier biochemical data (using subcellular fractionation analysis in vitro) and microscopic evidence (using filipin as the cholesterol stain), demonstrating that in cells containing the NPC1 mutation, cholesterol accumulated in late endosomal/lysosomal compartments. We therefore consider this possibility unlikely.] This interpretation is consistent with the observation made by Slot and colleagues (36), who used electron microscopy and flow cytometry to examine PM cholesterol staining by BCθ; they noted a sharp reduction of BCθ staining signal at the cell surface when cells were prefixed with PFA. To explain this result, they suggested that the binding between BCθ and membrane cholesterol may be inhibited by steric hindrance induced by crosslinking of membrane proteins when cells were fixed with PFA (36). Since PFA fixation seems to cause deformation/reorganization of the PM, it would not be appropriate to use the BCθ staining method or the filipin staining to quantitate the relative distribution of cholesterol between the PM and the cell interior.

To quantitate the fluorescent signals, we performed flow cytometric analysis of BCθ-stained CHO cells grown in lipoprotein-containing medium. As a negative control, we used RA cells incubated with fluorescent streptavidin alone without BCθ. As additional controls, we also included the WT CHO cells and mutant M19 cells in all of the experiments. The RA and CT cells contain a gain-of-function mutation in the protein SCAP (13). This property enables these cells to express the LDL receptor (LDLR) and various cholesterol biosynthetic enzymes at elevated levels constitutively. In contrast, the M19 cells lack the S2P gene that is essential for activating the SREBP pathway (41, 45). This property causes the M19 cells to express the

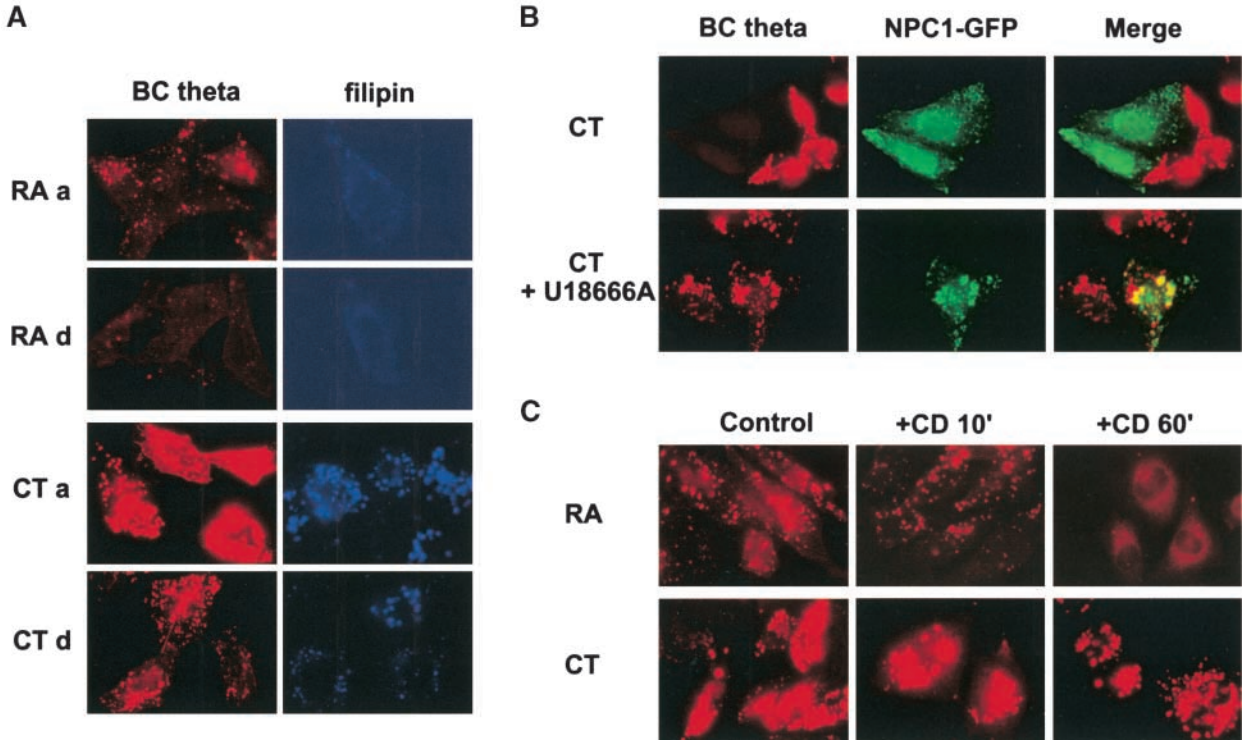


**Fig. 2.** Intracellular staining of Chinese hamster ovary (CHO) cells by BCθ in various conditions. In all cases, cells were fixed with 4% PFA, treated with BCθ, then secondarily labeled with Texas Red X streptavidin. A: Comparing BCθ staining signal with filipin staining signal. RA and CT cells were grown in medium A, then incubated in either medium A (a) or medium D (d) for 16 h. Cells were then processed for BCθ staining (left column) or for filipin staining (right column), and viewed under fluorescence microscopy. B: Effect of Niemann-Pick type C1 (NPC1) expression on BCθ staining in CT cells. CT cells were transiently transfected with green fluorescent protein (GFP) tagged NPC1 protein. Two days after transfection, cells were grown in the presence (lower panels) or absence (upper panels) of 2 μg/ml U18666A for 24 h before BCθ staining. Cells were viewed under fluorescence microscopy using the red channel (for BCθ signal) or the green channel (for GFP signal). In the upper panel, the two cells positive for GFP-tagged NPC1 protein (NPC1-GFP) expression were negative for the BCθ signal, in contrast to their neighboring cells (positive for the BCθ signal and negative for NPC1-GFP expression). In the bottom panel (treated with U18666A), the one cell positive for NPC1-GFP expression was still positive for the BCθ signal. The significant overlap between sites of the BCθ signal (red) and the those of the NPC1-GFP signal (green) is seen in yellow. C: Effect of cyclodextrin on BCθ staining in RA and CT cells. Cells were grown in medium A, and then incubated with 4% 2-hydroxypropyl-CD in medium D for 10 min (+CD 10′) or 60 min (+CD 60′) before BCθ staining. Control cells were not incubated with CD. The camera exposure times used for recording the upper frames or the lower frames in fluorescence microscopy were one-half and one-eighth sec, respectively. The pictures shown in A–C are representatives of a large number of cells randomly selected for photography.

LDLR and various cholesterol biosynthetic enzymes at levels significantly lower than those in the WT cells. Thus, grown in lipoprotein-containing medium, the RA cells and CT cells are expected to have a higher PM cholesterol content than the WT cells, while the M19 cells are expected to have a lower PM cholesterol content than the WT cells. The graph obtained from live-cell staining showed that indeed both RA and CT cells exhibited stronger fluorescence intensities than the WT cells, while the M19 cells exhibited weaker fluorescence intensities than the WT cells (Fig. 1B; results tabulated in **Table 1**, 3rd column). The results tabulated in Table 1, column 4, also showed that the RA cells and CT cells had greater percentages of cells with a strong positive signal than the WT cells, while the M19 cells had a much lower percentage of cells exhibiting a strong positive signal than the WT cells. We also noted that the average fluorescence signal was slightly higher in CT cells than in RA cells. This observation was consistently seen in three separate experiments. These results suggest that the bulk PM cholesterol content may not be significantly altered in the CT cells. We next performed additional flow cytometric experiments on cells stained with BCθ using RA, CT, WT, and M19 cells prefixed with 1% PFA, or with 4% PFA. The quantitation is shown in the second and third rows of Table 1. Under the 1% PFA fixation condition (where cell surface staining is dominant; Fig. 1A), CT cells still showed slightly higher levels of BCθ staining signal than those of RA cells or the WT cells, while the M19 cells showed the least amount of BCθ staining signal. Under the 4% PFA fixation condition, higher percentages of strong positive cells were observed in all four cell types. The intensity of the BCθ signal was considerably stronger in CT cells; it decreased in RA cells, WT cells, and M19 cells in sequential order. This result supports the interpretation that under this condition, most of the signal comes from staining of cholesterol accumulated intracellularly, and indicate that under the 4% PFA fixing condition, CHO cells become suitable for intracellular staining using BCθ without the need for any additional permeabilization procedure. Various conventional procedures, including treating cells with digitonin, methanol, or other detergents, could be employed to permeabilize cells; however, these procedures may not be able to preserve cholesterol-rich domain(s) present intracellularly.

### Comparing BCθ staining signal with filipin staining signal

To compare the BCθ staining with filipin staining, we grew RA and CT cells in medium A (containing FBS) or in medium D (containing delipidated FBS), performed parallel labeling experiments, then viewed cells using fluorescence microscopy. When cells were grown in medium A, BCθ was able to stain intracellular cholesterol in both RA and CT cells, with CT cells exhibiting a considerably greater signal (**Fig. 2A**; 1st and 3rd frames on the left). In contrast, filipin was able to stain intracellular cholesterol in CT cells but not in RA cells (Fig. 2A; 1st and 3rd frames on the right). When cells were incubated in the medium containing delipidated FBS (medium D) for 16 h, intracellular cholesterol content was reduced in both the RA cells and the CT cells, as shown by BCθ staining (Fig. 2A; left frames). Under the same conditions, filipin staining could show the decrease in intracellular cholesterol content in CT cells, but not in RA cells (Fig. 2A; right frames). These results demonstrate that BCθ is superior to filipin for staining cholesterol-rich domains in intracellular organelles. In additional experiments, we found that sequential incubations of BCθ followed by filipin completely abolished the filipin signal in NPC1 cells, implying that filipin may be targeted to the same cholesterol-rich domains intracellularly as BCθ is (data not shown).

### Effect of NPC1 expression on intracellular BCθ staining of CT cells

To examine the effect of NPC1 expression on intracellular BCθ staining in CT cells, we prepared a construct that

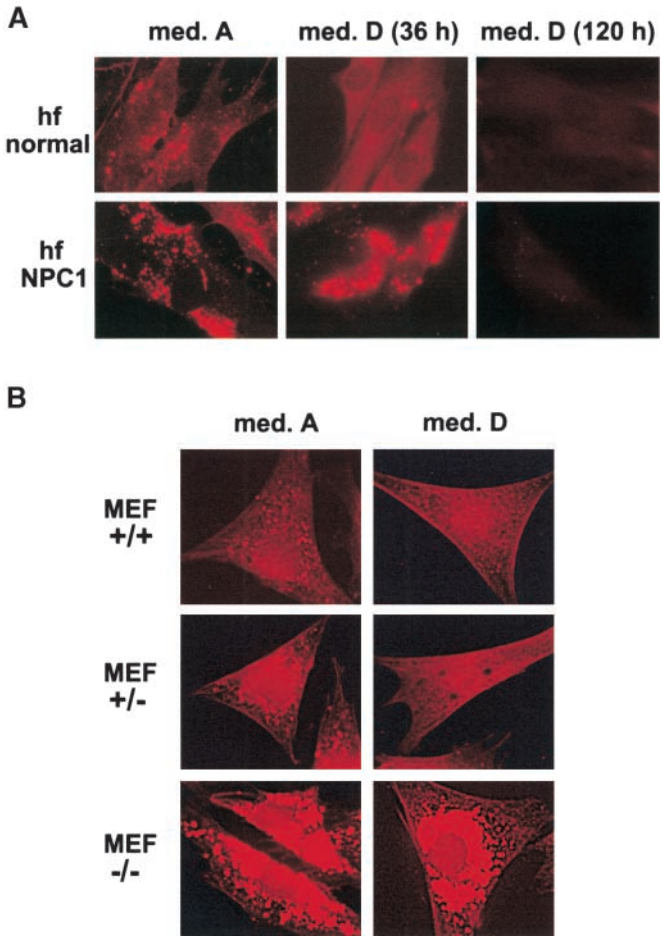


**Fig. 3.** Intracellular BCθ stainings of human fibroblasts and mouse embryonic fibroblasts. In all cases, cells were fixed with 4% PFA, treated with BCθ, then secondarily labeled with Texas Red X streptavidin. The samples were viewed under fluorescence microscopy. The pictures shown are representative of a large number of cells randomly selected for photography. A: Normal (hf Normal) and mutant NPC1 human fibroblasts (NPC1 93.22; hf NPC1) were grown in medium A or medium D for 36 h, or in medium D for 120 h before BCθ staining. B: WT ($^{+/+}$), heterozygous NPC1 ($^{+/-}$), and homozygous NPC1 ($^{-/-}$) mouse embryonic fibroblasts were isolated and grown in medium A or in medium D for 48 h before BCθ staining.

consists of an NPC1-GFP, and introduced it into CT cells by transient transfection. Previously, NPC1-GFP has been used as a tool to study the trafficking and function of the NPC1 protein in transfected cells (46, 47). After BCθ staining, the same cells were viewed in the red channel (for viewing the BCθ signal) or in the green channel (for viewing the NPC1-GFP signal); the two signals were then merged to examine their degree of overlap. As shown in the upper frames of Fig. 2B, cells expressing NPC1-GFP exhibit a significantly reduced BCθ staining signal compared with cells that do not express the fusion protein; no overlap was observed between the red and green channels. As a control, CT cells expressing only GFP did not show reduced BCθ staining (data not shown). U18666A is a polyamine-containing compound that induces an NPC-like phenotype when added to cells expressing a normal NPC1 (18, 48). When U18666A was incubated with CT cells that express the NPC1-GFP, the intracellular cholesterol staining by BCθ persisted (Fig. 2B; bottom two frames from the left). Merging these two frames showed that the BCθ staining significantly overlapped with the GFP signal (Fig. 2B; bottom frame from the right). Thus, the intracellular cholesterol-rich domain visualized by BCθ staining significantly colocalized with the compartment(s) that contains the NPC1-GFP in U18666A-treated cells. Previously, Strauss, Blanchette-Mackie, and colleagues, who used filipin as the intracellular cholesterol stain (49), made the same observation. It has been suggested that U18666A creates the NPC-like phenotype by "freezing" the NPC1 protein on the surface of cholesterol-laden lysosomes (47). The results described in Fig. 2B thus reinforce the conclusion that the cholesterol-rich compartment(s) stained by BCθ in NPC1 cells is probably the same compartment(s) stained by filipin.

### Effect of cyclodextrin on intracellular BCθ staining of RA and CT cells

β-Cyclodextrin (CD) is a cyclic oligosaccharide that specifically and rapidly removes free cholesterol from the cell membranes when added in the growth media (50). We used BCθ staining to study the change in the intracellular distribution of cholesterol in RA and CT cells treated with hpCD. Upon treating cells with 4% hpCD for 10 min, both cell lines retained most of the BCθ signals, suggesting that under this condition, only cholesterol at the cell surface is easily accessible to CD. When the CD incubation time was prolonged to 60 min, RA cells exhibited much less BCθ signal, whereas CT cells still retained much of the signal (Fig. 2C). These results suggest that the intracellular cholesterol pool in RA cells is relatively sensitive to CD extraction, while most of the intracellular cholesterol pool in CT cells is relatively resistant to CD extraction. Thus, the new method can be used to monitor the intracellular cholesterol removal process in a visual manner.

### Intracellular BCθ stainings in other cell types

To extend our findings in cells other than the CHO cells, we performed intracellular BCθ stainings in human and mouse fibroblasts. Both normal and NPC1 human fibroblasts grown in medium A exhibited intracellular cholesterol staining, with much greater signals present in the NPC1 cells (**Fig. 3A**; left frames). When cells were incubated with medium D for 36 h, normal cells lost most of the BCθ staining signal, while the NPC1 cells retained much of the signal (Fig. 3A; middle frames). When cells were incubated with medium D for 120 h, the staining signal was essentially cleared in both cell types. We also examined the intracellular BCθ stainings in embryonic fibroblasts isolated from normal, $NPC^{+/-}$, or $NPC^{-/-}$ mice. Fibroblasts grown in medium A showed intensities of intracellular BCθ staining in the order of $NPC1^{-/-} > NPC1^{+/-} > NPC1^{+/+}$ (Fig. 3B; left frames). When cultured in medium D for 48 h, both the $NPC1^{+/+}$ cells and $NPC1^{+/-}$ cells lost much of the BCθ staining signal. In contrast, the $NPC1^{-/-}$ fibroblasts still retained much of the signal.

Regarding the nature of binding between BCθ and the cholesterol-rich domains inside the cells, at present we do not know whether BCθ binds to cholesterol present in the phospholipid bilayer of the vesicles, or binds to the cholesterol-phospholipid complex within the vesicles. Despite this reservation, we have demonstrated a method for staining cholesterol-rich domains intracellularly in various NPC cells that is much more sensitive than the filipin staining method. For future work, we will use BCθ as a tool to study various cholesterol trafficking events inside the normal and NPC cells in a visual manner. The application of this methodology may help the investigators understand cellular cholesterol metabolism and trafficking processes under various normal and pathophysiological conditions.

The authors thank Song Lin for assistance with fluorescence microscopy, and Cathy Chang for her assistance and helpful discussion over the course of this work. The authors also thank Helina Morgan for carefully editing the manuscript. Confocal microscopy was performed at Dartmouth Medical School in The Herbert C. Englert Cell Analysis Laboratory, which was established by equipment grants from the Fannie E. Rippel Foundation and the National Institutes of Health Shared Instrument Program. Its operation is supported in part by the Core Grant (CA 23108) from the National Cancer Institute to the Norris Cotton Cancer Center. Y.S. is a Domestic Research Fellow of the Japan Science and Technology Corporation. This work was supported by National Institutes of Health Grants HL-36709 to T-Y.C. and NS-40564 to R.A.M.

## REFERENCES

1. Simons, K., and E. Ikonen. 2000. How cells handle cholesterol. *Science.* **290:** 1721–1726.
2. Mayor, S., S. Sabharanjak, and F. R. Maxfield. 1998. Cholesterol-dependent retention of GPI-anchored proteins in endosomes. *EMBO J.* **17:** 4626–4638.
3. Grimmer, S., T. G. Iversen, B. van Deurs, and K. Sandvig. 2000. Endosome to Golgi transport of ricin is regulated by cholesterol. *Mol. Biol. Cell.* **11:** 4205–4216.
4. Miwako, I., A. Yamamoto, T. Kitamura, K. Nagayama, and M. Ohashi. 2001. Cholesterol requirement for cation-independent mannose 6-phosphate receptor exit from multivesicular late endosomes to the Golgi. *J. Cell Sci.* **114:** 1765–1776.

5. Puri, V., R. Watanabe, M. Dominguez, X. Sun, C. L. Wheatley, D. L. Marks, and R. E. Pagano. 1999. Cholesterol modulates membrane traffic along the endocytic pathway in sphingolipid-storage diseases. *Nat. Cell Biol.* **1:** 386–388.
6. Puri, V., R. Watanabe, R. D. Singh, M. Dominguez, J. C. Brown, C. L. Wheatley, D. L. Marks, and R. E. Pagano. 2001. Clathrin-dependent and -independent internalization of plasma membrane sphingolipids initiates two Golgi targeting pathways. *J. Cell Biol.* **154:** 535–547.
7. Patterson, M. C., M. T. Vanier, K. Suzuki, J. A. Morris, E. Carstea, E. B. Neufeld, J. E. Blanchette-Mackie, and P. G. Pentchev. 2001. Niemann-Pick disease type C: A lipid trafficking disorder. *In* The Metabolic and Molecular Bases of Inherited Disease. C. R. Scriver, A. L. Beaudet, W. S. Sly and D. Valle, editors. McGraw-Hill, New York. 3611–3633.
8. Ioannou, Y. A. 2001. Multidrug permeases and subcellular cholesterol transport. *Nat. Rev. Mol. Cell Biol.* **2:** 657–668.
9. Cadigan, K. M., D. M. Spillane, and T. Y. Chang. 1990. Isolation and characterization of Chinese hamster ovary cell mutants defective in intracellular low density lipoprotein-cholesterol trafficking. *J. Cell Biol.* **110:** 295–308.
10. Gu, J. Z., E. D. Carstea, C. Cummings, J. A. Morris, S. K. Loftus, D. Zhang, K. G. Coleman, A. M. Cooney, M. E. Comly, L. Fandino, C. Roff, D. A. Tagle, W. J. Pavan, P. G. Pentchev, and M. A. Rosenfeld. 1997. Substantial narrowing of the Niemann-Pick C candidate interval by yeast artificial chromosome complementation. *Proc. Natl. Acad. Sci. USA.* **94:** 7378–7383.
11. Dahl, N. K., K. L. Reed, M. A. Daunais, J. R. Faust, and L. Liscum. 1992. Isolation and characterization of Chinese hamster ovary cells defective in the intracellular metabolism of low density lipoprotein-derived cholesterol. *J. Biol. Chem.* **267:** 4889–4896.
12. Chang, T. Y., and J. S. Limanek. 1980. Regulation of cytosolic acetoacetyl coenzyme A thiolase, 3-hydroxy-3-methylglutaryl coenzyme A synthase, 3-hydroxy-3-methylglutaryl coenzyme A reductase, and mevalonate kinase by low density lipoprotein and by 25-hydroxycholesterol in Chinese hamster ovary cells. *J. Biol. Chem.* **255:** 7787–7795.
13. Hua, X., A. Nohturfft, J. L. Goldstein, and M. S. Brown. 1996. Sterol resistance in CHO cells traced to point mutation in SREBP cleavage-activating protein. *Cell.* **87:** 415–426.
14. Cruz, J. C., and T. Y. Chang. 2000. Fate of endogenously synthesized cholesterol in Niemann-Pick type C1 cells. *J. Biol. Chem.* **275:** 41309–41316.
15. Cruz, J. C., S. Sugii, C. Yu, and T. Y. Chang. 2000. Role of Niemann-Pick type C1 protein in intracellular trafficking of low density lipoprotein-derived cholesterol. *J. Biol. Chem.* **275:** 4013–4021.
16. Pentchev, P. G., M. E. Comly, H. S. Kruth, M. T. Vanier, D. A. Wenger, S. Patel, and R. O. Brady. 1985. A defect in cholesterol esterification in Niemann-Pick disease (type C) patients. *Proc. Natl. Acad. Sci. USA.* **82:** 8247–8251.
17. Byers, D. M., M. W. Morgan, H. W. Cook, F. B. Palmer, and M. W. Spence. 1992. Niemann-Pick type II fibroblasts exhibit impaired cholesterol esterification in response to sphingomyelin hydrolysis. *Biochim. Biophys. Acta.* **1138:** 20–26.
18. Lange, Y., J. Ye, M. Rigney, and T. Steck. 2000. Cholesterol movement in Niemann-Pick type C cells and in cells treated with amphiphiles. *J. Biol. Chem.* **275:** 17468–17475.
19. Norman, A. W., R. A. Demel, B. de Kruyff, and L. L. van Deenen. 1972. Studies on the biological properties of polyene antibiotics. Evidence for the direct interaction of filipin with cholesterol. *J. Biol. Chem.* **247:** 1918–1929.
20. Miller, R. G. 1984. The use and abuse of filipin to localize cholesterol in membranes. *Cell Biol. Int. Rep.* **8:** 519–535.
21. Robinson, J. M., and M. J. Karnovsky. 1980. Evaluation of the polyene antibiotic filipin as a cytochemical probe for membrane cholesterol. *J. Histochem. Cytochem.* **28:** 161–168.
22. Severs, N. J., and H. L. Simons. 1983. Failure of filipin to detect cholesterol-rich domains in smooth muscle plasma membrane. *Nature.* **303:** 637–638.
23. Behnke, O., J. Tranum-Jensen, and B. van Deurs. 1984. Filipin as a cholesterol probe. II. Filipin-cholesterol interaction in red blood cell membranes. *Eur. J. Cell Biol.* **35:** 200–215.
24. Pelletier, R. M., and M. L. Vitale. 1994. Filipin vs enzymatic localization of cholesterol in guinea pig, mink, and mallard duck testicular cells. *J. Histochem. Cytochem.* **42:** 1539–1554.
25. Frolov, A., A. Petrescu, B. P. Atshaves, P. T. So, E. Gratton, G. Serrero, and F. Schroeder. 2000. High density lipoprotein-mediated cholesterol uptake and targeting to lipid droplets in intact L-cell fibroblasts. A single- and multiphoton fluorescence approach. *J. Biol. Chem.* **275:** 12769–12780.
26. Mukherjee, S., X. Zha, I. Tabas, and F. R. Maxfield. 1998. Cholesterol distribution in living cells: fluorescence imaging using dehydroergosterol as a fluorescent cholesterol analog. *Biophys. J.* **75:** 1915–1925.
27. Waheed, A. A., Y. Shimada, H. F. Heijnen, M. Nakamura, M. Inomata, M. Hayashi, S. Iwashita, J. W. Slot, and Y. Ohno-Iwashita. 2001. Selective binding of perfringolysin O derivative to cholesterol-rich membrane microdomains (rafts). *Proc. Natl. Acad. Sci. USA.* **98:** 4926–4931.
28. Iwamoto, M., I. Morita, M. Fukuda, S. Murota, S. Ando, and Y. Ohno-Iwashita. 1997. A biotinylated perfringolysin O derivative: a new probe for detection of cell surface cholesterol. *Biochim. Biophys. Acta.* **1327:** 222–230.
29. Ohno-Iwashita, Y., M. Iwamoto, S. Ando, K. Mitsui, and S. Iwashita. 1990. A modified theta-toxin produced by limited proteolysis and methylation: a probe for the functional study of membrane cholesterol. *Biochim. Biophys. Acta.* **1023:** 441–448.
30. Ohno-Iwashita, Y., M. Iwamoto, K. Mitsui, S. Ando, and S. Iwashita. 1991. A cytolysin, theta-toxin, preferentially binds to membrane cholesterol surrounded by phospholipids with 18-carbon hydrocarbon chains in cholesterol-rich region. *J. Biochem. (Tokyo).* **110:** 369–375.
31. Ohno-Iwashita, Y., M. Iwamoto, S. Ando, and S. Iwashita. 1992. Effect of lipidic factors on membrane cholesterol topology–mode of binding of theta-toxin to cholesterol in liposomes. *Biochim. Biophys. Acta.* **1109:** 81–90.
32. Nakamura, M., N. Sekino, M. Iwamoto, and Y. Ohno-Iwashita. 1995. Interaction of theta-toxin (perfringolysin O), a cholesterol-binding cytolysin, with liposomal membranes: change in the aromatic side chains upon binding and insertion. *Biochemistry.* **34:** 6513–6520.
33. Rossjohn, J., S. C. Feil, W. J. McKinstry, R. K. Tweten, and M. W. Parker. 1997. Structure of a cholesterol-binding, thiol-activated cytolysin and a model of its membrane form. *Cell.* **89:** 685–692.
34. Ohno-Iwashita, Y., M. Iwamoto, K. Mitsui, H. Kawasaki, and S. Ando. 1986. Cold-labile hemolysin produced by limited proteolysis of theta-toxin from Clostridium perfringens. *Biochemistry.* **25:** 6048–6053.
35. Hagiwara, H., S. Y. Kogure, M. Nakamura, Y. Shimada, Y. Ohno-Iwashita, and T. Fujimoto. 1999. Cross-linking of plasmalemmal cholesterol in lymphocytes induces capping, membrane shedding, and endocytosis through coated pits. *Biochem. Biophys. Res. Commun.* **260:** 516–521.
36. Mobius, W., Y. Ohno-Iwashita, E. G. van Donselaar, V. M. Oorschot, Y. Shimada, T. Fujimoto, H. F. Heijnen, H. J. Geuze, and J. W. Slot. 2002. Immunoelectron microscopic localization of cholesterol using biotinylated and non-cytolytic perfringolysin O. *J. Histochem. Cytochem.* **50:** 43–55.
37. Cadigan, K. M., J. G. Heider, and T. Y. Chang. 1988. Isolation and characterization of Chinese hamster ovary cell mutants deficient in acyl-coenzyme A: cholesterol acyltransferase activity. *J. Biol. Chem.* **263:** 274–282.
38. Shimada, Y., M. Nakamura, Y. Naito, K. Nomura, and Y. Ohno-Iwashita. 1999. C-terminal amino acid residues are required for the folding and cholesterol binding property of perfringolysin O, a pore-forming cytolysin. *J. Biol. Chem.* **274:** 18536–18542.
39. Willnow, T. E., and J. Herz. 1994. Genetic deficiency in low density lipoprotein receptor-related protein confers cellular resistance to Pseudomonas exotoxin A. Evidence that this protein is required for uptake and degradation of multiple ligands. *J. Cell Sci.* **107:** 719–726.
40. Henderson, L. P., L. Lin, A. Prasad, C. A. Paul, T. Y. Chang, and R. A. Maue. 2000. Embryonic striatal neurons from Niemann-Pick type C mice exhibit defects in cholesterol metabolism and neurotrophin responsiveness. *J. Biol. Chem.* **275:** 20179–20187.
41. Chin, J., and T. Y. Chang. 1981. Evidence for coordinate expression of 3-hydroxy-3-methylglutaryl coenzyme A. Reductase and low density lipoprotein binding activity. *J. Biol. Chem.* **256:** 6304–6310.
42. Liu, X., S. N. Constantinescu, Y. Sun, J. S. Bogan, D. Hirsch, R. A. Weinberg, and H. F. Lodish. 2000. Generation of mammalian cells stably expressing multiple genes at predetermined levels. *Anal. Biochem.* **280:** 20–28.
43. Fujimoto, T., M. Hayashi, M. Iwamoto, and Y. Ohno-Iwashita. 1997.

Crosslinked plasmalemmal cholesterol is sequestered to caveolae: analysis with a new cytochemical probe. *J. Histochem. Cytochem.* **45:** 1197–1205.
44. Hao, M., S. X. Lin, O. J. Karylowski, D. Wustner, T. E. McGraw, and F. R. Maxfield. 2002. Vesicular and non-vesicular sterol transport in living cells. The endocytic recycling compartment is a major sterol storage organelle. *J. Biol. Chem.* **277:** 609–617.
45. Rawson, R. B., N. G. Zelenski, D. Nijhawan, J. Ye, J. Sakai, M. T. Hasan, T. Y. Chang, M. S. Brown, and J. L. Goldstein. 1997. Complementation cloning of S2P, a gene encoding a putative metalloprotease required for intramembrane cleavage of SREBPs. *Mol. Cell.* **1:** 47–57.
46. Ko, D. C., M. D. Gordon, J. Y. Jin, and M. P. Scott. 2001. Dynamic movements of organelles containing Niemann-Pick C1 protein: NPC1 involvement in late endocytic events. *Mol. Biol. Cell.* **12:** 601–614.
47. Zhang, M., N. K. Dwyer, D. C. Love, A. Cooney, M. Comly, E. Neufeld, P. G. Pentchev, E. J. Blanchette-Mackie, and J. A. Hanover. 2001. Cessation of rapid late endosomal tubulovesicular trafficking in Niemann-Pick type C1 disease. *Proc. Natl. Acad. Sci. USA.* **98:** 4466–4471.
48. Liscum, L., and J. R. Faust. 1989. The intracellular transport of low density lipoprotein-derived cholesterol is inhibited in Chinese hamster ovary cells cultured with 3-beta-[2-(diethylamino) ethoxy]androst-5-en-17-one. *J. Biol. Chem.* **264:** 11796–11806.
49. Watari, H., E. J. Blanchette-Mackie, N. K. Dwyer, G. Sun, J. M. Glick, S. Patel, E. B. Neufeld, P. G. Pentchev, and J. F. Strauss 3rd. 2000. NPC1-containing compartment of human granulosa-lutein cells: a role in the intracellular trafficking of cholesterol supporting steroidogenesis. *Exp. Cell Res.* **255:** 56–66.
50. Rothblat, G. H., M. de la Llera-Moya, V. Atger, G. Kellner-Weibel, D. L. Williams, and M. C. Phillips. 1999. Cell cholesterol efflux: integration of old and new observations provides new insights. *J. Lipid Res.* **40:** 781–796.